Journal of Poultry Sciences and Avian Diseases

Journal homepage: www.jpsad.com

Effect of Green Nano Cineole and Green Nano Silver on Altering the Expression of Caspase 3 and NFkB in Kidney Cells Exposed with Ochratoxin A: Implications for Poultry Health

Saeid Razzaghi Khezerloo[1], Alireza Khosravi[1*], Donya Nikaein[1], Hesameddin Akbarein[2], Javad Malakootikhah[3]

[1] Department of Microbiology and Immunology Faculty of Veterinary Medicine, University of Tehran, Tehran, Iran
[2] Department of Food Hygiene, Faculty of Veterinary Medicine, University of Tehran, Tehran, Iran
[3] Researcher and PhD Graduation in Nanobiotechnology of University of Tehran, Tehran, Iran

*** Corresponding author email address**: Khosravi@ut.ac.ir

A r t i c l e I n f o

Article type:
Original Research

How to cite this article:
Razzaghi Khezerloo, S., Khosravi, A., Nikaein, D., Akbarein, H., & Malakootikhah, J. (2026). Effect of Green Nano Cineole and Green Nano Silver on Altering the Expression of Caspase 3 and NFkB in Kidney Cells Exposed with Ochratoxin A: Implications for Poultry Health. *Journal of Poultry Sciences and Avian Diseases, 4*(1), 1-11.
http://dx.doi.org/10.61838/kman.jpsad.150

A B S T R A C T

Ochratoxin A (OTA) is a biologically produced mycotoxin with nephrotoxic, hepatotoxic, and immunotoxic properties, commonly generated by various Aspergillus and Penicillium species. The aim of this study was to evaluate the toxicological effects of OTA on human kidney cells by analyzing the expression of inflammation-related genes (Caspase-3 and NF-κB), and to investigate the individual and combined effects of silver nanoparticles (AgNPs) and nano-cineole on the expression of these genes. The cell viability of OTA-treated and untreated HEK-293 cells was assessed using the MTT assay. HEK-293 cells treated with AgNPs, cineole nanoparticles, and their combination, as well as OTA-induced HEK-293 cells, were used to study the expression of genes involved in the apoptotic pathway, particularly Caspase-3 and NF-κB. Apoptosis was also evaluated using the Annexin V apoptosis detection kit. The MTT assay results indicated a significant decrease in cell viability in HEK-293 cells exposed to OTA. Conversely, treatment with higher concentrations of both AgNPs and nano-cineole significantly improved cell viability. qPCR analysis showed that treatment with all nanoparticle types (individual and combined) significantly reduced the expression of Caspase-3 and NF-κB genes in OTA-exposed cells (p<0.05). The percentage of apoptotic cells was lower in nanoparticle-treated groups compared to OTA-only treated cells, suggesting that these nanoparticles can mitigate OTA-induced cytotoxicity. These findings may also have implications for poultry health, as ochratoxin A is a common contaminant in poultry feed, and similar cellular pathways are involved in toxin-induced kidney damage in poultry.

Keywords: *Ochratoxin A; Poultry; Apoptosis; HEK-293 cell line; Silver nanoparticles; Nano-cineole*

Article history:
Received 17 July 2025
Revised 19 September 2025
Accepted 30 September 2025
Published online 01 January 2026

1 Introduction

Mycotoxins are secondary metabolites produced by toxigenic fungi that can contaminate various food products. Ochratoxin A (OTA), a biologically synthesized mycotoxin, exhibits nephrotoxic, hepatotoxic, and immunotoxic properties and is mainly produced by *Aspergillus* and *Penicillium* species (1). Due to its ubiquity, biological origin, and chemical stability, OTA can be produced and persist throughout food storage and transportation, making human exposure to this toxin inevitable. Studies have shown that mycotoxins can damage specific cells by reducing cell viability, inducing apoptosis and autophagy, and causing cell cycle arrest.

In addition to human health concerns, OTA contamination is a major issue in poultry production systems. Poultry feed is frequently contaminated with ochratoxin-producing fungi, leading to nephrotoxicity, immunosuppression, poor growth performance, and increased susceptibility to infectious diseases in broiler chickens and laying hens (2, 3). Considering the economic importance of the poultry industry and the critical role of feed safety in flock health, exploring novel mitigation strategies such as green-synthesized nanoparticles could have valuable implications for both veterinary and public health.

Reactive oxygen species (ROS) are highly reactive by-products of normal cellular metabolism. Excessive ROS production leads to oxidative stress, which in turn contributes to apoptosis and cell cycle disruption (4). OTA has been shown to enhance ROS generation, resulting in apoptosis in normal cells (5, 6). The European Food Safety Authority has classified OTA as a potent nephrotoxin in animals such as rodents and pigs, with kidney damage severity being dose and duration-dependent. OTA-induced genotoxicity is believed to stem from the generation of free radicals, leading to cellular injury and renal carcinogenesis observed in murine models (7).

To improve food safety and prolong shelf life, developing novel antimicrobial agents is necessary. One promising strategy involves the use of antimicrobial compounds, either directly applied to food or incorporated into packaging materials (8). Recently, there has been increased interest in using inorganic antimicrobial agents in food and non-food applications (9). Among these, silver nanoparticles (AgNPs) and 1,8-cineole have demonstrated considerable antimicrobial efficacy (Lima et al., 2021)(10). AgNPs have widely become used due to their potent antibacterial and antifungal activities.

Gómez et al. (2019) demonstrated the ability of engineered AgNPs to inhibit mycotoxins such as aflatoxins and OTA, as well as the growth of major mycotoxigenic fungi including *Aspergillus flavus*, *A. parasiticus*, *A. carbonarius*, *A. niger*, *A. ochraceus*, *A. steynii*, *A. westerdijkiae*, and *Penicillium verrucosum (*11*)*. Similarly, Khalil et al. (2019) reported the anti-mycotoxin activity of biogenic AgNPs synthesized by *Fusarium chlamydosporum* and *Penicillium chrysogenum*, even at non-cytotoxic levels (12). AgNPs are known to induce apoptosis in fibroblast cells via ROS production and JNK pathway activation, leading to mitochondria-dependent cell death (13). Furthermore, AgNPs can modulate TNF-α signaling, promoting inflammation through the NF-κB and cytokine pathways (14).

Natural phytochemicals such as 1,8-cineole have shown the ability to modulate cellular and humoral immune responses. This monoterpene, commonly used in food, cosmetics, and pharmaceuticals due to its aroma and flavor, possesses insecticidal, antibacterial, hepatoprotective, and anti-inflammatory properties (15). However, its therapeutic potential is limited by poor water solubility and low stability. To overcome these limitations, nano-based formulations of cineole have been developed. Previous studies have reported that 1,8-cineole exhibits stronger antifungal and anti-ochratoxigenic activity against A. carbonarius compared to other essential oils, such as those from Lavandula dentata and Laurus nobilis (16). Linghu et al. (2016) demonstrated that 1,8-cineole ameliorates cellular dysfunction by suppressing NF-κB activation (15). Additionally, cineole has been found to induce mitochondrial stress and activate caspases, leading to programmed cell death in normal cells (17)(Nikbakht Rad et al., 2022).

Therefore, the aim of the present study was to investigate the synergistic effects of silver nanoparticles and nano-cineole on OTA-induced cytotoxicity in human kidney cells (HEK-293 cell line) by evaluating the expression levels of inflammation-related genes Caspase-3 and NF-κB

2 Materials and Methods

2.1 Preparation and characterization of Nanoparticles

To prevent oxidation of the silver nitrate solution, 0.169 g of $AgNO_3$ was dissolved in 1 L of deionized water to prepare a 1 mM silver nitrate solution (Merck, Germany). The solution was stored in an amber-colored container to

protect it from light. Silver nanoparticles (AgNPs) were synthesized via a one-step method. Briefly, 90 mL of silver nitrate solution and 10 mL of cineole solution (Merck, Germany) were mixed and heated to 80 °C for 15 minutes. The solution color changed from pale yellow to brown, indicating the formation of AgNPs. The produced nanoparticles were then stored for 24 hours in a 12 N hydrochloric acid solution. AgNPs were separated from the mixture by centrifugation and repeatedly washed with distilled water until all hydrochloric acid residues were removed (18).

The 1,8-cineole powder used to synthesize cineole nanoparticles (cineol-NPs) was purchased from Merck (Germany). Cineol-NPs were prepared using a physicochemical method as described by Hettiarachchi et al. (2021). The stock cineole solution (5 mg/mL) was prepared by dissolving cineole powder in 20 mL of dichloromethane. Under ultrasonication (Velp Scientifica, Europe), 1 mL of the stock solution was added dropwise into 50 mL of boiling water at a flow rate of 0.1 mL/min. The mixture was sonicated for 30 minutes and then stirred at 800 rpm for 20 minutes until a precipitate formed. The supernatant was discarded, and the cineol-NPs were collected for further analysis (19).

Topological, morphological, and compositional analyses were performed using a Nova Nano FE-SEM 450 (FEI) scanning electron microscope (SEM). The instrument operated with beam landing energies from 30 keV to 50 eV, offering resolutions of 1.4 nm at 1 kV and 1 nm at 15 kV. Prior to SEM analysis, all nanoparticles were coated with gold. Dynamic light scattering (DLS) and Zeta-potential measurements were carried out using a Zeta Sizer (Nano-ZS, Malvern Instruments Ltd., UK). For these analyses, 5 mg of the samples were dissolved in 30 mL of distilled water and sonicated for 15 minutes. The resulting colloidal solution was diluted 1:1 with distilled water, sonicated again, and used for particle size distribution and Zeta-potential measurement. All experiments were performed in triplicate

2.2 Cell Culture

The HEK293 cells were obtained from the Iranian Biological Resource Center (Tehran, Iran). HEK293 cells were grown in DMEM/F12+ Glutamax HEPES culture mix with 10% FBS (Gibco, USA) and 100 U/mL antibiotics (Penicillin and Streptomycin) (SigmaAldrich, USA) in a 5% CO_2 incubator (BINDER, USA) at 37°C. The cells reached around 75% confluence and were transferred to 96-well plates and 25-cm^2 flasks based on the experimental setup.

2.3 MTT assay

The effects of nanoparticles on the proliferation and survival of normal and OTA-induced HEK-293 cells were evaluated using the MTT Cell Viability Assay Kit (DNAbiotech Company, Iran) following the manufacturer's protocol. HEK-293 cells were treated with silver nanoparticles (AgNPs) and green cineole nanoparticles for 24 hours before performing the MTT assay. For the assay, 100 µL of complete culture medium containing 10^5 HEK-293 cells and 100 µL of each nanoparticle concentration (100, 50, 25, 12.5, 6.5, 3.125, 1.56, 0.78, 0.39, and 0.195 µg/mL) were added to individual wells of a 96-well plate. Well 11 served as the positive control, and well 12 was used as the negative control.

Next, 100 µL of working MTT solution was added to each well, and the plate was incubated at 37 °C for 4 hours. Subsequently, 100 µL of acidified isopropanol buffer was added to each well, and the plate was incubated for an additional 15 minutes at 37 °C. Absorbance was measured at 570 nm (with a 690 nm reference filter) using a SpectraFluor microplate reader (Tecan, Crailsheim, Germany). All tests were performed in triplicate (18).

To assess the effects of AgNPs and green cineole nanoparticles on OTA-induced HEK-293 cells, 1 mL of complete DMEM medium was added to six wells of a culture plate. Subsequently, 200 µL of green cineole nanoparticles and 250 µL of AgNPs at concentrations ranging from 1 to 10 µg/mL were added to the cells. Ten µg/mL of OTA was applied to the wells to induce toxicity (18). At the end of treatments, 10^5 cells were seeded into each well. Four experimental groups were designed for cytotoxicity evaluation:

- Group 1: HEK-293 cells treated with AgNPs
- Group 2: HEK-293 cells treated with cineole nanoparticles
- Group 3: OTA-induced HEK-293 cells treated with AgNPs
- Group 4: OTA-induced HEK-293 cells treated with cineole nanoparticles

The experiments were repeated twice, with plates incubated for 18 hours at 37 °C in a humidified atmosphere containing 5% CO_2. Cell viability percentage was calculated using the following formula

$$\text{Percentage of viability} = 100 \times \frac{\text{Absorption (treated} - \text{well)}}{\text{Absorption (control} - \text{well)}}$$

2.4 *RNA extraction and RT-PCR*

Total RNA was extracted from HEK-293 cells, OTA-induced HEK-293 cells, AgNPs-treated cells, and cineole nanoparticle-treated cells using the TRIsure reagent (Bioline, Luckenwalde, Germany) according to the manufacturer's instructions. RNA concentration and purity were assessed by measuring absorbance at 260/280 nm using a NanoDrop One UV-Vis Spectrophotometer (Thermo Fisher Scientific, Waltham, MA, USA). RNA integrity was confirmed by electrophoresis on 1% agarose gel.

Complementary DNA (cDNA) synthesis was performed using the BioFact™ RT Series cDNA synthesis kit with reverse transcriptase enzyme. Quantitative real-time PCR (qRT-PCR) was subsequently conducted as a one-step process with the QuantiTect SYBR Green Kit (Qiagen) on a Rotor-Gene RG-3000 instrument. Primer sequences for *Caspase 3*, *NF-κB*, and *GAPDH* genes were obtained from previous studies and are presented in Table 1. Primer specificity was confirmed by melting curve analysis. Relative gene expression was calculated using the 2^−ΔΔCt method with *GAPDH* as the internal reference gene.

Table 1. Gene-specific primers used.

	Primer Sequence (5'- 3')	
Gene	Forward	Reverse
caspase-3	CATGGAAGCGAATCAATGGACT	CTGTACCAGACCGAGATGTCA
NF-kB	ATCCCATCTTTGACAATCGTGC	CTGGTCCCGTGAAATACACCTC
GAPDH	GCACCGTCAAGGCTGAGAAC	TGGTGAAGACGCCAGTGGA

2.5 *Apoptosis detection by flow cytometry*

Apoptosis rates in HEK-293 cells and OTA-induced HEK-293 cells treated with nanoparticles were assessed using the Annexin-V Apoptosis Detection Kit (MabTag) following the manufacturer's protocol. HEK-293 cells were cultured in T25 flasks and treated with the IC_{50} concentrations of AgNPs, cineole nanoparticles, and combined nanoparticles for 24 hours.

Cells were then harvested from each flask, and pellets from control and treated groups were resuspended in 90 µL of 1× Annexin-V binding buffer. Subsequently, 5 µL of Annexin-V conjugate and 5 µL of propidium iodide (PI) solution were added to each tube, followed by incubation in the dark for 20 minutes. Afterward, 400 µL of Annexin-V binding buffer was added.

Following centrifugation at 400 × g for 5 minutes, cells were resuspended in 1× Annexin-V binding buffer and analyzed for apoptotic cell death using a BD FACS Calibur flow cytometer (BD Biosciences, San Jose, CA, USA). Flow cytometry data were processed with FlowJo v10 CL software (Manufacturer) (18).

2.6 *Statistical analysis*

The experimental data were presented as Mean±SEM, calculated using GraphPad Prism 6 software. Three replicates were conducted to establish the standard deviation. The data were analyzed using one-way ANOVA followed by Tukey's post-hoc test to determine statistically significant differences between the groups, with a significance level set at $p<0.05$.

3 Results

3.1 *NPs morphology and size*

The particle size, Polydispersity index (PDI), and Zeta-potential of the synthesized NPs were investigated using DLS. According to the results, green AgNPs and combined NPs had an average size of 128.3 ± 10.8, and 169.3 ± 8.4, PDI of 0.079 and 0.212 and Zeta potential of -19.2 and -31.4 (mV), respectively (Figure 1). The shape, size, morphology, and surface texture of the AgNPs, Cineole NPs and combined form of NPs were detected using the SEM technique. The SEM of prepared NPs further suggested their smooth surface texture, and spherical polydisperse particles with a mean diameter of approximately 20-100 nm (Figure 2).

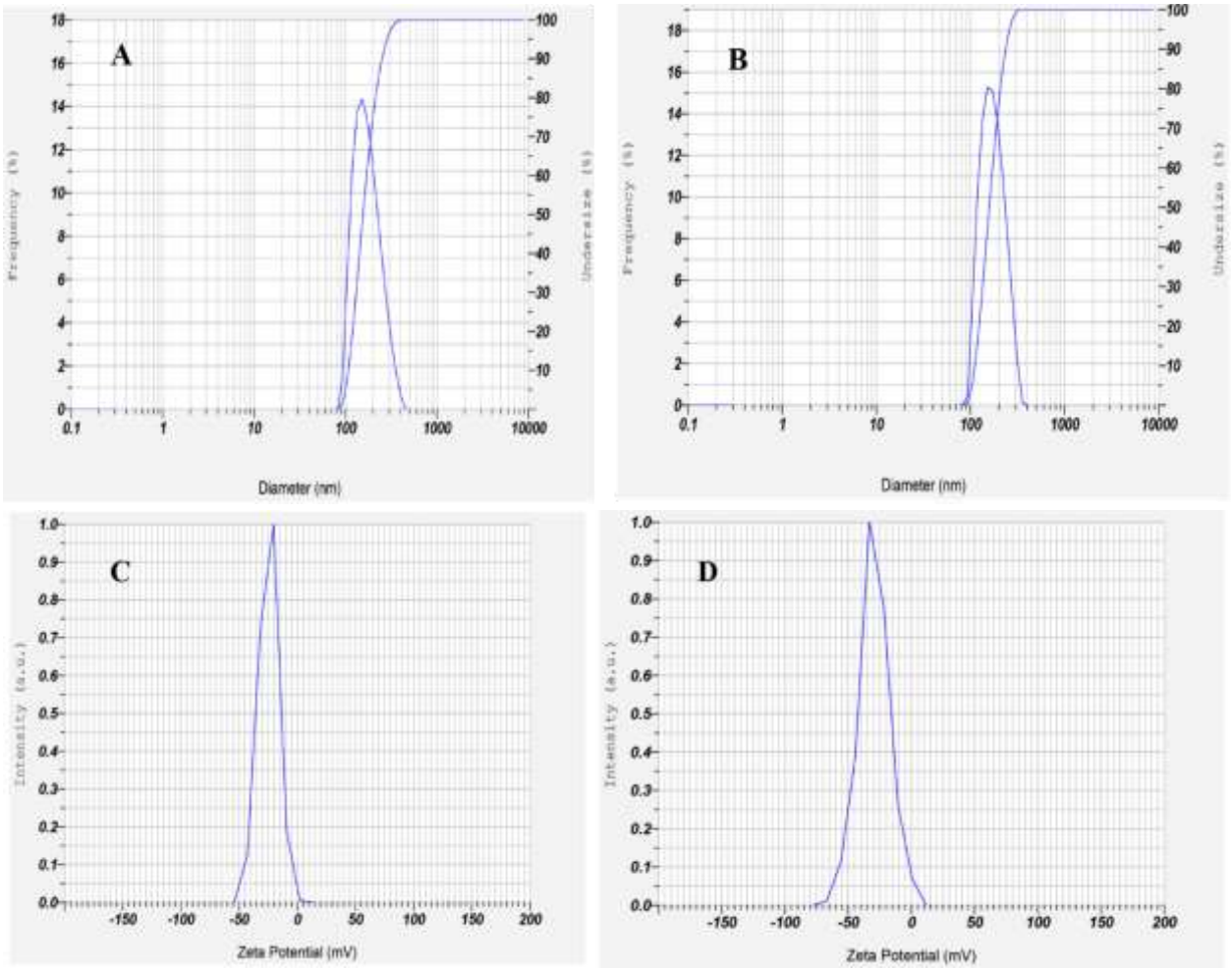

Figure 1. Dynamic light scattering (DLS) analysis of the synthesized nanoparticles. (A) Size distribution curve of green AgNPs; (B) size distribution curve of combined NPs; (C) Zeta potential distribution of green AgNPs; and (D) Zeta potential distribution of combined NPs.

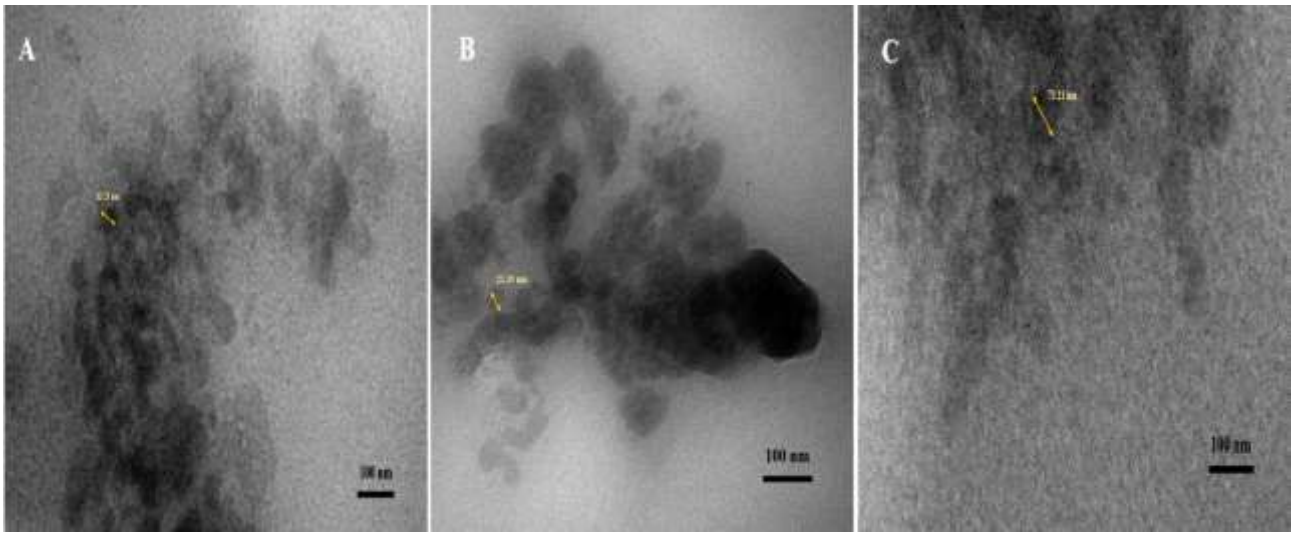

Figure 2. . Scanning electron micrographs (SEM) of the synthesized nanoparticles showing the morphology and surface structure of (A) green AgNPs, (B) Cineole NPs, and (C) the combined form of NPs. All samples display predominantly spherical particles with smooth surface texture.

3.2 Cytotoxic activity

The cytotoxic effects of AgNPs and Cineole nanoparticles on both untreated and OTA-treated HEK-293 cells were assessed using the MTT assay after 21 hours of exposure (Figure 3). A concentration-dependent cytotoxicity pattern was observed in normal HEK-293 cells exposed to higher concentrations of both AgNPs and Cineole nanoparticles (100, 50, 25, 12.5, 6.25, 3.125, and 1.56 µg/mL), with a reduction in cell viability of up to 40% at 100 µg/mL compared to the control group. In contrast, no significant cytotoxicity was detected at lower concentrations (0.78, 0.39, and 0.195 µg/mL), indicating a safer profile at these doses.

Exposure to OTA alone led to a marked decline in cell viability, confirming its high toxicity to human kidney cells. However, when OTA-induced HEK-293 cells were treated with increasing concentrations of AgNPs or Cineole nanoparticles (from 3.125 to 100 µg/mL), a notable improvement in cell viability was observed. Remarkably, treatment with the lowest nanoparticle concentrations (0.39 and 0.195 µg/mL) restored cell viability in OTA-induced cells to nearly 100%.

These results suggest that high concentrations of nanoparticles may exert cytotoxic effects on healthy cells, whereas low concentrations of the same nanoparticles can alleviate OTA-induced cytotoxicity and promote cell survival.

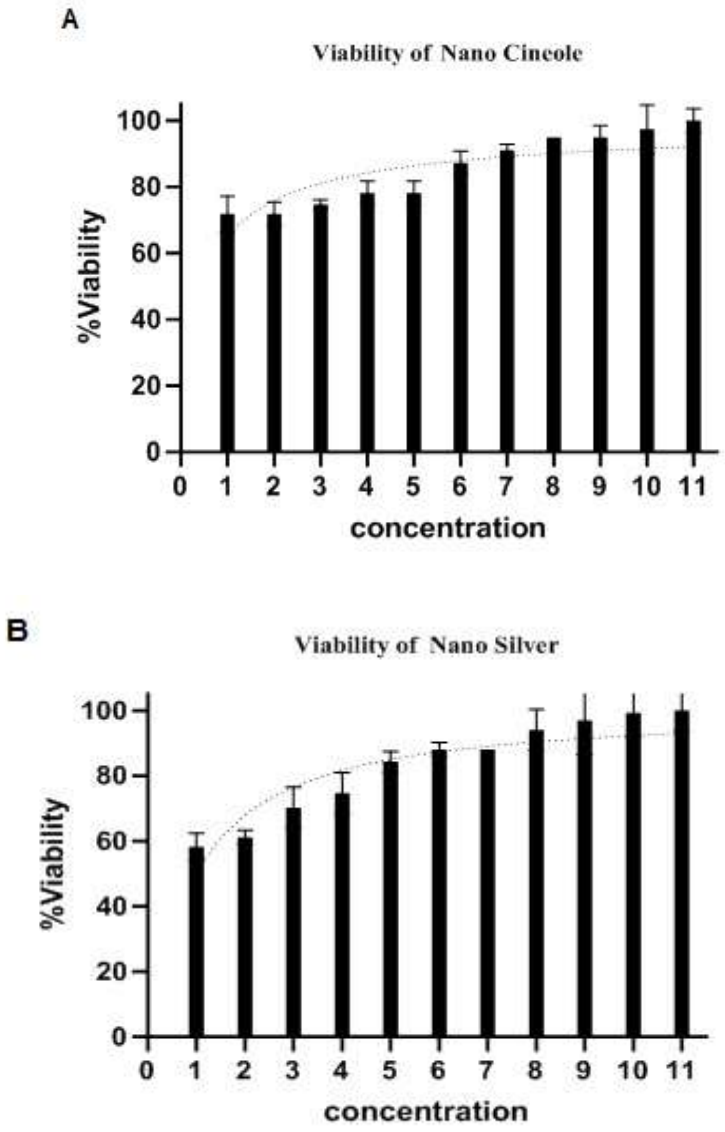

Figure 3. A) HEK-293 cell viability treated with cineole nanoparticles. B) HEK-293 cell viability treated with AgNPs.

3.3 *Caspase 3 and NFkB genes expression*

The expression levels of Caspase 3 and NF-κB, two critical genes involved in the apoptosis and inflammation pathways, were evaluated in untreated HEK-293 cells, OTA-induced HEK-293 cells, and cells treated with AgNPs, Cineole nanoparticles, or their combination (Figure 4). Quantitative PCR analysis revealed a significant downregulation of both Caspase 3 and NF-κB gene expression in OTA-induced cells treated with all nanoparticle forms compared to untreated OTA-induced cells (p<0.001).

The combined treatment exhibited the most substantial inhibitory effect on Caspase 3 and NF-κB expression in normal HEK-293 cells relative to the control group (p<0.001). However, in OTA-induced cells, while the combination therapy did not significantly alter Caspase 3 expression compared to OTA-only cells, it significantly reduced the expression of NF-κB (p<0.001).

Furthermore, the reduction in gene expression was more pronounced in cells treated with Cineole nanoparticles alone than in those treated with AgNPs, suggesting that Cineole nanoparticles are more effective in mitigating OTA-induced cellular damage through downregulation of apoptotic and inflammatory pathways.

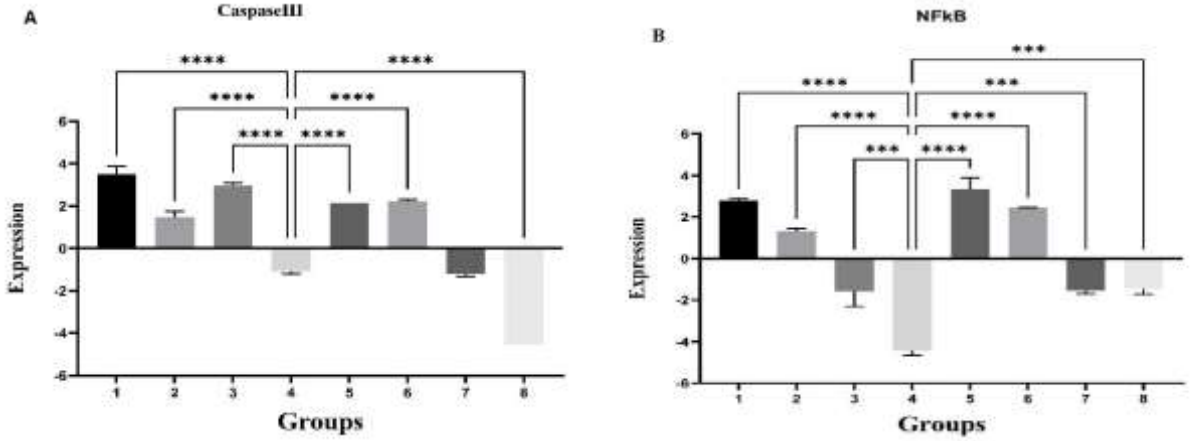

Figure 4. (A) Caspase 3 and (B) NFκB gene expression in HEK-293 and OTA-induced HEK-293 cells treated with AgNPs, cineole nanoparticles, and combined-NPs. The groups are as follows: (1) Cell + OTA, (2) Cell + OTA + Nano Cineole, (3) Cell + OTA + Nano Silver, (4) Control, (5) Cell + Nano Cineole, (6) Cell + Nano Silver, (7) Cell + OTA + Nano Cineole + Nano Silver, and (8) Cell + Nano Cineole + Nano Silver. Data are presented as Mean±SEM. Statistical significance is indicated as **** (p<0.0001)

3.4 *Flow cytometry analysis*

Flow cytometric analysis was performed to evaluate the effects of AgNPs, cineole nanoparticles, and their combination on apoptosis in both untreated and OTA-induced HEK-293 cells (Figure 5). A marked increase in apoptotic cell populations was observed following treatment with all nanoparticle forms and OTA compared to untreated control cells.

In normal HEK-293 cells, baseline levels of early and late apoptosis were 2.8% and 1.9%, respectively. Treatment with cineole nanoparticles resulted in 64.7% early and 10.0% late apoptotic cells, while AgNPs induced 13.5% early and 49.4% late apoptosis. Combined nanoparticle treatment led to 57.3% early and 19.2% late apoptosis. These findings indicate that nanoparticle exposure induces apoptosis even in untreated cells, with variations depending on nanoparticle type.

In OTA-induced HEK-293 cells, early and late apoptosis rates reached 10.8% and 69.6%, respectively, indicating significant OTA-induced cytotoxicity. However, following treatment with cineole nanoparticles, these rates decreased to 55.6% and 19.3%, respectively. AgNPs treatment led to 11.6% early and 53.0% late apoptosis, while combined nanoparticles reduced apoptosis levels to 52.4% (early) and 24.3% (late).

Overall, these results suggest that both cineole and silver nanoparticles—particularly when combined—can mitigate

OTA-induced cytotoxicity by reducing apoptosis rates. Furthermore, the combination therapy appeared to lessen the necrotic effects observed in cells treated with AgNPs alone, indicating a possible protective interaction between the two nanoparticle types.

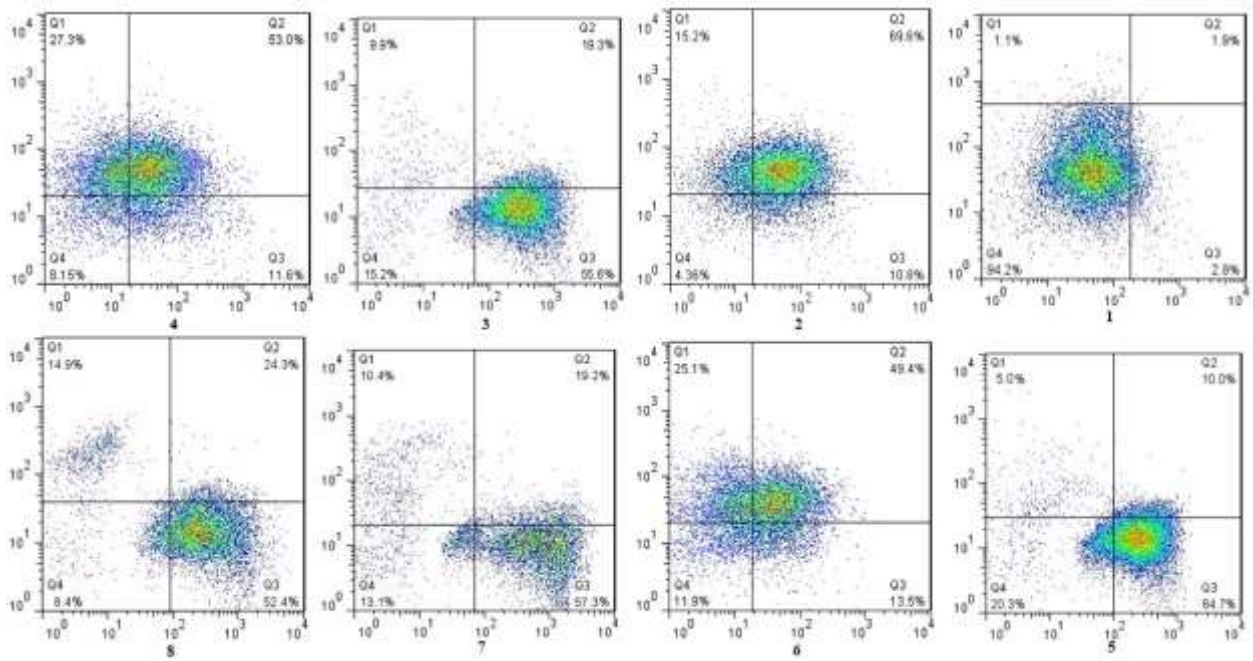

Figure 5. Figure 5. Flow cytometry plots for the impact of exposure to AgNPs, cineole nanoparticles, and combination nanoparticles on the death of HEK-293 cells and OTA-induced HEK-293 cells.

4 Discussion

The results showed that treatment with increased concentrations of both AgNPs and cineole nanoparticles significantly enhanced the viability of OTA-induced HEK-293 cell lines and reduced the toxic effects of OTA on normal cells. Numerous studies have indicated that exposure to OTA in both in vitro and in vivo systems results in excessive generation of free radicals, leading to oxidative damage to lipids, proteins, and DNA (1, 4). OTA is known to trigger lipid peroxidation by utilizing Fe3+ as a cofactor. The NADPH-CYP450 reductase-OTA-Fe3+ complex facilitates the reduction of Fe3+ to Fe2+, leading to the formation of the OTA-Fe2+ complex, which promotes free radical generation, lipid peroxidation, and DNA damage (5).

This oxidative stress could explain why normal cells lose viability following OTA exposure. Damiano et al. (2018) identified oxidative stress as a key contributor to OTA-induced kidney damage and proposed δ-tocotrienol as a potential antioxidant to mitigate this effect (20). Curcumin has also been shown to reduce the adverse effects of chronic OTA exposure by modulating inflammatory markers, reducing nitric oxide levels, and minimizing oxidative DNA damage in kidney and liver tissues (21).

Nanoparticles such as zinc oxide, silver, gold, selenium, and carbon-based materials possess notable antioxidant properties (8, 9) (Lima et al., 2021). Green-synthesized nanoparticles are particularly enriched in natural bioactive compounds, enhancing their antioxidant capabilities (10). Mao et al. (2022) reported that supplementation with selenomethionine significantly reduced OTA-induced cytotoxicity in MDCK cells (18). Similarly, Abdel-Wahhab et al. (2017) demonstrated that chitosan nanoparticles combined with quercetin alleviated oxidative stress and DNA damage in the kidneys of rats fed OTA-contaminated diets (7).

ZnONPs synthesized via green methods have been shown to improve pathological outcomes of OTA toxicity, including tissue degeneration, vascular congestion, and necrosis in liver and kidney tissues (9). Biogenic AgNPs were also effective in reducing aflatoxin and OTA production by Aspergillus strains without harming normal human melanocytes (12). Selenium nanoparticles exhibited potent antifungal activity, inhibiting OTA production by

Aspergillus ochraceus and *Penicillium verrucosum*, and displayed strong biocompatibility with normal cell lines.

OTA has been shown to induce both apoptotic and necrotic cell death (4). Markers of apoptosis such as DNA fragmentation, chromatin condensation, and caspase-3 activation have been observed even at nanomolar concentrations (14). The results showed that the combination of cineole and AgNPs exerted the most profound effects on the expression of Caspase 3 and NF-kB genes in normal cells, suggesting it as the most effective treatment to prevent OTA-induced cell death.

Significant changes in gene transcription related to apoptosis were observed following OTA exposure (15). ASK1 has been identified as a key regulator in the activation of JNK and p38 pathways during oxidative and ER stress, mediating OTA-induced cell death (22). Furthermore, OTA increased the expression of inflammatory mediators such as TNF-α and IL-6, implying the involvement of the NF-kB pathway (23).

Several biological agents have been shown to counteract OTA-induced damage by activating the Nrf2 pathway, which protects against oxidative stress. Selenomethionine at 8 µM inhibited OTA-induced NLRP3 inflammasome activation and pyroptosis (18). Li et al. (2021) demonstrated that low-dose fumonisin B1 enhanced OTA-induced nephrotoxicity and pro-apoptotic gene expression in PK-15 cells, which was mitigated by NAC and a JNK inhibitor (SP600125). NAC reduced the expression of p-JNK, thereby counteracting the combined toxin effects.

OTA also suppresses AKT, PI3K, and Bcl-2 pathways, while increasing the expression of Caspase 3, Bax, and P53. Selenium yeast improved antioxidant defense via activation of the Nrf2/Keap1 pathway, reversing the downregulation of Nrf2 target genes such as HO-1 and MnSOD (1). Huang et al. (2021) also reported that OTA induces embryotoxicity by disrupting mitochondrial membrane potential and activating caspases, effects that were alleviated by liquiritigenin (24).

Flow cytometry confirmed that OTA increased apoptosis and necrosis in HEK-293 cells. However, combination treatment with cineole and AgNPs significantly reduced apoptotic and necrotic events. Additionally, bioinspired AgNPs disrupted membrane permeability in fungal cells and inhibited OTA and aflatoxin synthesis at concentrations below 8 µg/mL, while showing minimal toxicity toward human fibroblasts (25).

AgNPs also cause surface protein and nucleic acid damage and interfere with proton pumps (26). They generate intracellular ROS, damage membrane proteins, and disrupt mitochondrial function, leading to apoptosis (13). AgNPs alter the expression of genes related to the TCA cycle, ergosterol biosynthesis, and lipid metabolism, compromising membrane integrity (23).

The present findings also hold significance beyond human cell models. In poultry, OTA exposure has been shown to impair kidney and liver function, disrupt immune responses, and alter gene expression related to apoptosis and inflammation (6, 27). Similar to human systems, activation of Caspase-3 and NF-κB pathways has been implicated in OTA-induced tissue damage in broiler chickens. Therefore, the observed mitigating effects of green nano-cineole and silver nanoparticles in the current study may provide a scientific foundation for future in vivo experiments in avian species. Such investigations could determine whether nanoparticle-based strategies can be translated into practical feed additives or therapeutic agents to reduce OTA-related economic losses in the poultry sector.

OTA was also shown to disrupt meiotic spindle formation and mitochondrial function, leading to oxidative stress, apoptosis, and autophagy. Melatonin ameliorated these effects and preserved oocyte integrity (28). Patial et al. (2022) reported that sea buckthorn leaf extract protected against OTA-induced renal damage in Japanese quail. Bacillus subtilis fermentation extract also mitigated oxidative stress, lipid peroxidation, and tissue damage caused by OTA exposure (29).

5 Conclusion

There are a few studies have been undertaken on the synergic impact of nanoparticles with phytochemicals on mycotoxin toxicity in normal cells. Therefore, the current work explored the combined effect of Ag-NPs with Cineole on the toxicity induced by OTA in HEK-293 cell line. Our paper The results indicated that green-synthesized AgNP, cineole nanoparticles, and their combination form are hazardous to normal HEK-293 cells. After treating normal cells with OTA, the application of produced nanoparticles and their combination resulted in enhanced survival of normal cells and reduced toxicity induced by OTA. The combination of AgNPs and cineole nanoparticles shows promise for utilizing nanoparticles to improve mycotoxin-induced toxicity in human cells. Additional research is needed to enhance this combination and determine the best application methods. Moreover, it is important to note that ochratoxin A exerts similar nephrotoxic and pro-inflammatory effects in a wide range of animal species,

including poultry, where it has been shown to upregulate inflammatory genes and impair kidney function. Therefore, findings of the present study may also provide a basis for future investigations on the potential use of nanoparticle-based strategies to mitigate OTA-induced toxicity in poultry

Acknowledgements

We would like to acknowledge and thank Yasouj University for its cooperation and assistance in conducting this research.

Conflict of Interest

All authors declare that they have no conflicts of interest.

Author Contributions

M. H., H. A and M. Kh. designed and directed the experiment, analyzed the data. A. R. and M. H. carried out the farm experiment, laboratory measurements and data collection. All authors participated in writing and reading the manuscript.

Data Availability Statement

The data that support the findings of this study are available from the corresponding author upon reasonable request.

Ethical Considerations

In conducting this study, ethical principles have been fully observed.

Funding

No funding was received for this research.

References

1. Li Y, Yi J, Zeng Q, Liu Y, Yang B, Liu B, et al. Zearalenone exposure mediated hepatotoxicity via mitochondrial apoptotic and autophagy pathways: Associated with gut microbiome and metabolites. Toxicology. 2021;462:152957. [PMID: 34537261] [DOI]
2. Huff WE, Kubena LF, Harvey RB, Phillips TD. Efficacy of hydrated sodium calcium aluminosilicate to reduce the individual and combined toxicity of aflatoxin and ochratoxin A. Poultry Science. 1988;67(4):586-92.
3. Stoev SD. Studies on carcinogenic and toxic effects of ochratoxin A in chicks. Toxins. 2010;2(4):649-64. [PMID: 22069604] [PMCID: PMC3153202] [DOI]
4. Wang Y, Cui J, Zheng G, Zhao M, Hao Z, Lian H, et al. Ochratoxin A induces cytotoxicity through ROS-mediated endoplasmic reticulum stress pathway in human gastric epithelium cells. Toxicology. 2022;479:153309. [PMID: 36058351] [DOI]
5. Tao Y, Xie S, Xu F, Liu A, Wang Y, Chen D. Ochratoxin A: Toxicity, oxidative stress and metabolism. Food and Chemical Toxicology. 2018;112:320-31. [PMID: 29309824] [DOI]
6. Wang J, Tang L, Li Y. Phytic acid alleviates ochratoxin A-induced renal damage in chicks. Food and Chemical Toxicology. 2024;182:113485. [DOI]
7. Abdel-Wahhab MA, Aljawish A, El-Nekeety AA, Abdel-Aziem SH, Hassan NS. Chitosan nanoparticles plus quercetin suppress the oxidative stress, modulate DNA fragmentation and gene expression in the kidney of rats fed ochratoxin A-contaminated diet. Food and Chemical Toxicology. 2017;99:209-21. [PMID: 27923682] [DOI]
8. Mouhamed AE, Hassan AA, Hassan M, El Hariri M, Refai M. Effect of metal nanoparticles on the growth of ochratoxigenic moulds and ochratoxin A production isolated from food and feed. International Journal of Research Studies in Biosciences. 2015;3(9):1-14.
9. Hassan SA, Mujahid H, Ali MM, Irshad S, Naseer R, Saeed S, et al. Synthesis, characterization and protective effect of green tea-mediated zinc oxide nanoparticles against ochratoxin A induced hepatotoxicity and nephrotoxicity in albino rats. Applied Nanoscience. 2021;11(8):2281-9. [DOI]
10. Schneider G. Antimicrobial silver nanoparticles-regulatory situation in the European Union. Materials Today: Proceedings. 2017;4:S200-S7. [DOI]
11. Gómez JV, Tarazona A, Mateo F, Jiménez M, Mateo EM. Potential impact of engineered silver nanoparticles in the control of aflatoxins, ochratoxin A and the main aflatoxigenic and ochratoxigenic species affecting foods. Food Control. 2019;101:58-68. [DOI]
12. Khalil NM, Abd El-Ghany MN. Antifungal and anti-mycotoxin efficacy of biogenic silver nanoparticles produced by Fusarium chlamydosporum and Penicillium chrysogenum at non-cytotoxic doses. Chemosphere. 2019;218:477-86. [PMID: 30497030] [DOI]
13. Hsin YH, Chen CF, Huang S, Shih TS, Lai PS, Chueh PJ. The apoptotic effect of nanosilver is mediated by a ROS- and JNK-dependent mechanism involving the mitochondrial pathway in NIH3T3 cells. Toxicology Letters. 2008;179(3):130-9. [PMID: 18547751] [DOI]
14. Fehaid A, Fujii R, Sato T, Taniguchi A. Silver nanoparticles affect the inflammatory response in a lung epithelial cell line. The Open Biotechnology Journal. 2020;14(1). [DOI]
15. Linghu K, Lin D, Yang H, Xu Y, Zhang Y, Tao L, et al. Ameliorating effects of 1,8-cineole on LPS-induced human umbilical vein endothelial cell injury by suppressing NF-κB signaling in vitro. European Journal of Pharmacology. 2016;789:195-201. [PMID: 27455900] [DOI]
16. Dammak I, Hamdi Z, El Euch SK, Zemni H, Mliki A, Hassouna M. Evaluation of antifungal and anti-ochratoxigenic activities of Salvia officinalis, Lavandula dentata and Laurus nobilis essential oils and a major monoterpene constituent 1,8-cineole against Aspergillus carbonarius. Industrial Crops and Products. 2019;128:85-93. [DOI]
17. Cha JD, Kim YH, Kim JY. Essential oil and 1,8-cineole from Artemisia lavandulaefolia induces apoptosis in KB cells via mitochondrial stress and caspase activation. Food Science and Biotechnology. 2010;19:185-91. [DOI]
18. Mao X, Li H, Ge L, Liu S, Hou L, Yue D, et al. Selenomethionine alleviated ochratoxin A-induced pyroptosis and renal fibrotic factor expressions in MDCK cells. Journal of Biochemical and Molecular Toxicology. 2022;36(1):e22933. [PMID: 34676619] [DOI]

19. Hettiarachchi SS, Dunuweera SP, Dunuweera AN, Rajapakse RG. Synthesis of curcumin nanoparticles from raw turmeric rhizome. ACS Omega. 2021;6(12):8246-52. [PMID: 33817483] [PMCID: PMC8015141] [DOI]
20. Damiano S, Navas L, Lombari P, Montagnaro S, Forte IM, Giordano A, et al. Effects of δ-tocotrienol on ochratoxin A-induced nephrotoxicity in rats. Journal of Cellular Physiology. 2018;233(11):8731-9. [PMID: 29775204] [DOI]
21. Longobardi C, Damiano S, Andretta E, Prisco F, Russo V, Pagnini F, et al. Curcumin modulates nitrosative stress, inflammation, and DNA damage and protects against ochratoxin A-induced hepatotoxicity and nephrotoxicity in rats. Antioxidants. 2021;10(8):1239. [PMID: 34439487] [PMCID: PMC8389288] [DOI]
22. Liang R, Shen XL, Zhang B, Li Y, Xu W, Zhao C. Apoptosis signal-regulating kinase 1 promotes ochratoxin A-induced renal cytotoxicity. Scientific Reports. 2015;5:8078. [PMID: 25627963] [PMCID: PMC5389036] [DOI]
23. Yi B, Hu X, Zhang H, Huang J, Liu J, Hu J. Nuclear NF-κB p65 in peripheral blood mononuclear cells correlates with urinary MCP-1, RANTES and the severity of type 2 diabetic nephropathy. PLoS ONE. 2014;9(6):e99633. [PMID: 24936866] [PMCID: PMC4061032] [DOI]
24. Huang Y, Zhang C, Li H, Gan F, Li J, Huang K. Liquiritigenin attenuates ochratoxin A-induced embryotoxicity and apoptosis by inhibiting ROS generation and mitochondrial dysfunction. Toxicology Research. 2021;10:999-1008.
25. Bryła M, Damaziak K, Twarużek M, Waśkiewicz A, Stępień Ł, Roszko M, et al. Toxico-pathological effects of ochratoxin A and its diastereoisomer under in ovo conditions and in vitro evaluation of the toxicity of these toxins against the embryo Gallus gallus fibroblast cell line. Poultry Science. 2023;102(2):102413. [PMID: 36566659] [PMCID: PMC9801203] [DOI]
26. Cheng W, Wu D, Zuo Q, Wang Z, Fan W. Ginsenoside Rb1 prevents interleukin-1 beta induced inflammation and apoptosis in human articular chondrocytes. International Orthopaedics. 2013;37(10):2065-70. [PMID: 23835558] [PMCID: PMC3779573] [DOI]
27. Kövesi B, Varga F, Kelet Z. Curcumin mitigates ochratoxin A-induced oxidative stress and alters gene expression in broiler chicken liver and kidney. Acta Veterinaria Hungarica. 2024;72(1):41-50. [PMID: 38536404] [DOI]
28. Lan M, Zhang Y, Wan X, Pan MH, Xu Y, Sun SC. Melatonin ameliorates ochratoxin A-induced oxidative stress and apoptosis in porcine oocytes. Environmental Pollution. 2020;256:113374. [PMID: 31672358] [DOI]
29. Elhady MA, Khalaf AAA, Ibrahim MA, Hassanen EI, Abdelrahman RE, Noshy PA. Protective effects of Bacillus subtilis fermentation extract against ochratoxin A-induced nephrotoxicity and immunotoxicity in broiler chickens. Journal of Veterinary Research. 2022;66(2):167-77. [PMID: 35892096] [PMCID: PMC9281517] [DOI]